



Calmodulin kinase II–mediated sarcoplasmic reticulum Ca²⁺ leak promotes atrial fibrillation in mice

Mihail G. Chelu,^{1,2} Satyam Sarma,^{1,3} Subeena Sood,¹ Sufen Wang,^{4,5} Ralph J. van Oort,¹ Darlene G. Skapura,¹ Na Li,¹ Marco Santonastasi,¹ Frank Ulrich Müller,⁶ Wilhelm Schmitz,⁶ Ulrich Schotten,⁷ Mark E. Anderson,⁸ Miguel Valderrábano,^{4,5} Dobromir Dobrev,⁹ and Xander H.T. Wehrens^{1,3}

¹Department of Molecular Physiology and Biophysics, Baylor College of Medicine, Houston, Texas, USA.

²Department of Internal Medicine, University of Texas Health Science Center, Houston, Texas, USA. ³Department of Medicine, Division of Cardiology, Baylor College of Medicine, Houston, Texas, USA. ⁴Department of Cardiology, The Methodist Hospital, Houston, Texas, USA.

⁵Division of Cardiology, Weill Medical College of Cornell University, New York, New York, USA. ⁶Institute of Pharmacology and Toxicology, University of Münster, Münster, Germany. ⁷Department of Physiology, Maastricht University, Maastricht, The Netherlands.

⁸Department of Internal Medicine, Division of Cardiovascular Medicine, and Department of Molecular Physiology and Biophysics, University of Iowa Carver College of Medicine, Iowa City, Iowa, USA. ⁹Department of Pharmacology and Toxicology, Dresden University of Technology, Dresden, Germany.

Atrial fibrillation (AF), the most common human cardiac arrhythmia, is associated with abnormal intracellular Ca²⁺ handling. Diastolic Ca²⁺ release from the sarcoplasmic reticulum via “leaky” ryanodine receptors (RyR2s) is hypothesized to contribute to arrhythmogenesis in AF, but the molecular mechanisms are incompletely understood. Here, we have shown that mice with a genetic gain-of-function defect in *Ryr2* (which we termed *Ryr2*^{R176Q/+} mice) did not exhibit spontaneous AF but that rapid atrial pacing unmasked an increased vulnerability to AF in these mice compared with wild-type mice. Rapid atrial pacing resulted in increased Ca²⁺/calmodulin-dependent protein kinase II (CaMKII) phosphorylation of RyR2, while both pharmacologic and genetic inhibition of CaMKII prevented AF inducibility in *Ryr2*^{R176Q/+} mice. This result suggests that AF requires both an arrhythmogenic substrate (e.g., RyR2 mutation) and enhanced CaMKII activity. Increased CaMKII phosphorylation of RyR2 was observed in atrial biopsies from mice with atrial enlargement and spontaneous AF, goats with lone AF, and patients with chronic AF. Genetic inhibition of CaMKII phosphorylation of RyR2 in *Ryr2*^{S281A} knockin mice reduced AF inducibility in a vagotonic AF model. Together, these findings suggest that increased RyR2-dependent Ca²⁺ leakage due to enhanced CaMKII activity is an important downstream effect of CaMKII in individuals susceptible to AF induction.

Introduction

Atrial fibrillation (AF) is the most common sustained cardiac arrhythmia and is a significant contributor to cardiovascular morbidity and possibly mortality. Emerging evidence suggests an important role for abnormal intracellular Ca²⁺ handling in atrial arrhythmogenesis. In cardiac myocytes, excitation-contraction coupling is governed by a mechanism known as Ca²⁺-induced Ca²⁺ release (1). The influx of Ca²⁺ via L-type voltage-gated Ca²⁺ channels (Cav1.2) (activates a much greater release of Ca²⁺ from the sarcoplasmic reticulum (SR) via ryanodine receptor type 2 (RyR2)/intracellular Ca²⁺ channels (2). The amplitude and kinetics of these

Ca²⁺ fluxes are tightly regulated in cardiac myocytes in order to ensure physiological modulation of contractility.

Atrial myocytes isolated from patients in chronic AF exhibit an increased incidence of spontaneous SR Ca²⁺ release events, which are thought to be proarrhythmogenic (3, 4). Since the amplitude of the L-type voltage-gated Ca²⁺ current is typically decreased in AF (5, 6), it has been postulated that these abnormal Ca²⁺ release events might be caused by enhanced activity of the RyR2 Ca²⁺ release channel (4, 7). Previous studies demonstrated higher single-channel open probabilities of RyR2 isolated from dogs in persistent AF at low cytosolic Ca²⁺ concentrations (4). Furthermore, biochemical studies revealed increased levels of PKA phosphorylation of RyR2 at S2808 and decreased FK506-binding protein 12.6-kDa (FKBP12.6; also known as calstabin2) levels in the channel macromolecular complex (4). These molecular changes may contribute to the failure of RyR2 channels to close completely during diastole, leading to Ca²⁺ leak from the SR (4), a phenomenon that is increasingly being recognized as an important contributor to arrhythmogenesis (8–10). However, the concept that SR Ca²⁺ leak due to gain-of-function defects in RyR2 – regardless of the underlying molecular basis – might predispose to AF remains somewhat controversial (11, 12).

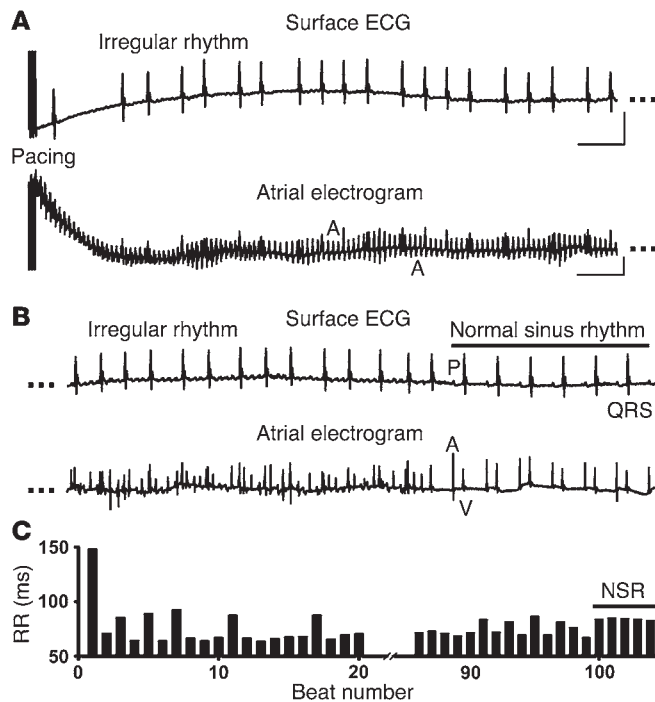
Important advances in our understanding of the pathogenesis of AF have been made using various large animal models of this disease, including the elucidation of changes in Ca²⁺-handling

Authorship note: Dobromir Dobrev and Xander H.T. Wehrens are co-senior authors. Mihail G. Chelu, Satyam Sarma, and Subeena Sood contributed equally to this work.

Conflict of interest: Mark E. Anderson is a named inventor on patents claiming to treat arrhythmias by CaMKII inhibition. All other authors have declared that no conflict of interest exists.

Nonstandard abbreviations used: AERP, atrial effective refractory period; AF, atrial fibrillation; BCL, basic cycle length; [Ca²⁺]_i, intracellular Ca²⁺ transient; CaMKII, Ca²⁺/calmodulin-dependent protein kinase II; Cav1.2, L-type voltage-gated Ca²⁺ channel; CL, cycle length; CREM, cAMP-response element modulator; NCX1, Na⁺/Ca²⁺ exchanger; PLN, phospholamban; PV, pulmonary vein; RyR2, ryanodine receptor type 2; SERCA2a, sarcoplasmic/endoplasmic reticulum Ca²⁺-ATPase; SR, sarcoplasmic reticulum.

Citation for this article: *J. Clin. Invest.* 119:1940–1951 (2009). doi:10.1172/JCI37059.

**Figure 1**

Ryr2^{R176Q/+} knockin mice are vulnerable to pacing-induced AF. (A) Representative surface ECG and intracardiac atrial electrogram showing pacing-induced AF in a *Ryr2*^{R176Q/+} knockin mouse. Surface ECG demonstrates lack of P waves and irregular RR intervals. Atrial electrogram displays rapid and irregular atrial electrical activity. Three dots indicate truncation of the recording. (B) Continuation of the surface ECG and intracardiac atrial electrogram from A showing transition from AF to normal sinus rhythm in a *Ryr2*^{R176Q/+} knockin mouse. P, P wave; QRS, QRS complex; A, atrial wave; V, ventricular wave. (C) Quantification of the RR interval for the beats represented in A and B showing RR variability during the irregular rhythm followed by regular RR interval during the normal sinus rhythm (NSR). Scale bar: 0.1 mV (vertical axis); 100 ms (horizontal axis).

Results

Increased susceptibility to pacing-induced AF in *Ryr2*^{R176Q/+} mice. Ambulatory ECGs were recorded in WT and *Ryr2*^{R176Q/+} knockin mice using telemetry. No episodes of spontaneous AF were observed in any of the *Ryr2*^{R176Q/+} or WT mice (Supplemental Figure 1; supplemental material available online with this article; doi:10.1172/JCI37059DS1). To test for AF inducibility, *Ryr2*^{R176Q/+} and WT mice were subjected to simultaneous surface ECG recordings and invasive electrophysiological studies at baseline and following high-frequency atrial burst pacing, as described by Verheule et al. (17).

Episodes of pacing-induced AF were observed more frequently in *Ryr2*^{R176Q/+} mice (58%, 18 of 31) than in WT mice (11%, 4 of 34; $P < 0.01$). AF episodes were characterized by the lack of P waves and a high degree of beat-to-beat RR interval variability in lead II of the surface ECG (Figure 1, A and B). RR intervals during AF ranged from 78 ms to 148 ms (Figure 1C). AF was confirmed by rapid and irregular A waves on the atrial electrogram (Figure 1, A and B). Mean duration of AF episodes in *Ryr2*^{R176Q/+} mice was 13.5 ± 3.4 seconds. All episodes of AF in *Ryr2*^{R176Q/+} mice returned spontaneously to sinus rhythm, as demonstrated by the return of P waves followed regularly by QRS complexes on surface ECG (Figure 1B). The transition to normal sinus rhythm was also confirmed by the recurrence of regular A waves followed by V waves in the atrial and atrioventricular electrogram (Figure 1B).

At baseline, 6-lead surface ECG and 4-lead bipolar intracardiac electrograms recorded simultaneously in *Ryr2*^{R176Q/+} and WT mice did not reveal any abnormalities such as atrial or ventricular arrhythmias or conduction delays (Supplemental Figure 1). There were no differences in heart rate, RR, PR, QRS, or corrected QT intervals on surface ECGs comparing *Ryr2*^{R176Q/+} and WT mice (Supplemental Table 1). These findings were corroborated by measuring the electrical properties of the conduction system of the heart using bipolar intracardiac electrogram recordings (Supplemental Figure 1). No significant differences between *Ryr2*^{R176Q/+} and WT mice were found in the sinus node recovery time, atrial effective refractory period (AERP), and atrioventricular nodal effective refractory period measured using endocardial programmed electrical stimulation at 100 ms basic cycle length (BCL) (Supplemental Table 1).

Pacing-induced enhancement of RyR2 phosphorylation at S2814 in *Ryr2*^{R176Q/+} mice. At baseline heart rates, levels of CaMKII-T287 autophosphorylation — which correlate well with cytosolic CaMKII δ activity (18) — were similar in *Ryr2*^{R176Q/+} and WT mice, suggesting that the R176Q mutation in RyR2 did not alter baseline CaMKII activity levels (Supplemental Figure 2). Because we have previously

proteins in dogs, goats, and pigs with remodeled atria due to chronic AF (13). However, studying the specific role of an RyR2 gain-of-function defect in the pathogenesis of AF requires an animal model in which this Ca²⁺ channel has been selectively perturbed. Therefore, we studied a recently established knockin mouse model with the R176Q mutation in the *Ryr2* gene, as this mutation was previously shown to cause SR Ca²⁺ leak after catecholaminergic stimulation associated with ventricular arrhythmias (14, 15). Despite the fact that the R176Q mutation in *Ryr2* increases its diastolic leakiness (16), spontaneous atrial arrhythmias were not observed in *Ryr2*^{R176Q/+} mice. However, *Ryr2*^{R176Q/+} mice did develop AF following rapid atrial pacing, suggesting the dual requirement for an arrhythmogenic substrate (e.g., RyR2 mutation) and a trigger activated by the faster heart rate. Our data show that rapid atrial pacing-associated activation of Ca²⁺/calmodulin-dependent protein kinase II (CaMKII) with subsequent CaMKII phosphorylation of RyR2 may amplify RyR2 leak, thereby providing the molecular basis of the trigger (rapid atrial pacing) of inducible AF episodes in this model. Consistent with this hypothesis, we demonstrate that pharmacologic and genetic inhibition of CaMKII prevents pacing-induced AF in *Ryr2*^{R176Q/+} mice. In atrial biopsies from goats with lone AF (structural heart disease absent) and from CREM-Ib Δ C-X (where CREM indicates *cAMP-response element modulator*) transgenic mice (which spontaneously develop AF in the presence of structural heart disease) or from patients with chronic AF (structural heart disease present), the levels of CaMKII phosphorylation of RyR2 were increased compared with those of control animals and sinus rhythm patients, respectively. Finally, genetic inhibition of CaMKII phosphorylation of RyR2 in *Ryr2*^{S2814A} knockin mice reduced AF inducibility in a vagotonic AF model. Thus, our data suggest that CaMKII-mediated enhancement of RyR2-dependent SR Ca²⁺ leak is an important, albeit not necessarily exclusive, factor involved in the initiation of clinical AF.

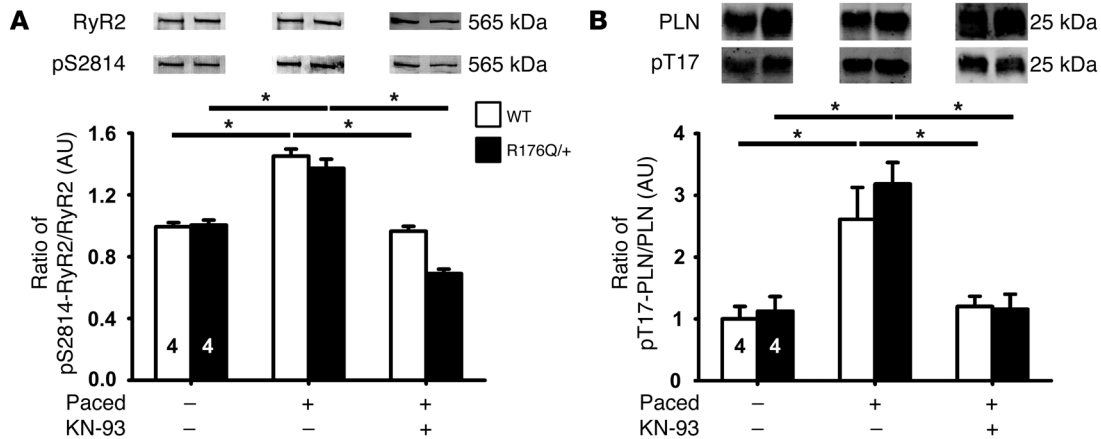


Figure 2

CaMKII inhibition prevents pacing-induced increase in RyR2 phosphorylation at S2814. (A) Representative Western blots of total RyR2 and S2814-phosphorylated RyR2 at baseline and after pacing in WT and *Ryr2*^{R176Q/+} (R176Q/+) atria nontreated or treated with the CaMKII inhibitor KN-93. Bar graph showing quantification of Western blots band densities. The ratios of pS2814-RyR2 density divided by RyR2 density presented in the bar graph represent average data of 4 mice in each group. (B) Representative Western blots of total PLN and T17-phosphorylated PLN at baseline and after pacing in WT and *Ryr2*^{R176Q/+} atria nontreated or treated with the CaMKII inhibitor KN-93. Bar graph showing quantification of Western blot band densities. The ratios of pT17-PLN density divided by PLN density presented in the bar graph represent average data of 4 mice in each group. **P* < 0.05, comparing indicated groups.

demonstrated that increasing the heart rate activates CaMKII and enhances CaMKII phosphorylation of RyR2 in ventricular myocardium (18), we subsequently determined whether rapid atrial pacing results in increased CaMKII phosphorylation of RyR2 at its specific phosphorylation site, S2814. Mice were intubated, the heart exposed using thoracotomy, and the right atrium paced using an intracardiac catheter as described above. Atrial samples were quickly excised and flash-frozen within seconds following the termination of atrial burst pacing to preserve RyR2 phosphorylation levels. Western blotting revealed a 50% increase in S2814 phosphorylation of RyR2 after pacing compared with baseline (*P* < 0.05) (Figure 2A). Pacing induced the same degree of increase in RyR2-phosphorylation levels at S2814 in WT and *Ryr2*^{R176Q/+} mice (Figure 2A). Moreover, pretreatment with CaMKII inhibitor KN-93 (30 μmol/kg, i.p.) prevented the pacing-induced increase of RyR2 phosphorylation at S2814 in both WT and *Ryr2*^{R176Q/+} mice (Figure 2A). Whereas atrial pacing enhanced CaMKII phosphorylation of RyR2 at S2814, phosphorylation levels of the (PKA) site S2808 were unaltered (Supplemental Figure 3).

Pacing-induced activation of CaMKII also resulted in enhanced phosphorylation of other downstream targets of CaMKII. Western blotting revealed an approximately 150% increase in T17 phosphorylation of phospholamban (PLN) after pacing as compared with baseline (*P* < 0.05) (Figure 2B). The increase in CaMKII phosphorylation of PLN at T17 following pacing was similar in *Ryr2*^{R176Q/+} and WT mice (Figure 2B). Pretreatment with CaMKII inhibitor KN-93 (30 μmol/kg, i.p.) prevented pacing-induced PLN phosphorylation in both *Ryr2*^{R176Q/+} and WT mice (Figure 2B). Increased CaMKII phosphorylation of PLN might contribute to arrhythmogenesis by increasing sarcoplasmic/endoplasmic reticulum Ca²⁺-ATPase (SERCA2a) activity, thereby enhancing SR Ca²⁺ loading. Taken together, these findings suggest that the level of CaMKII activation and resulting phosphorylation of Ca²⁺-handling proteins were similar in *Ryr2*^{R176Q/+} and WT mice under resting conditions and that rapid atrial pacing produced a similar

increase in CaMKII activity with comparable phosphorylation levels of RyR2 and PLN in *Ryr2*^{R176Q/+} and WT mice.

Suppression of AF inducibility by pharmacological and genetic inhibition of CaMKII in Ryr2^{R176Q/+} mice. To determine whether the increased AF susceptibility in *Ryr2*^{R176Q/+} mice was mediated by CaMKII activation induced by fast pacing, we repeated the atrial burst protocol in *Ryr2*^{R176Q/+} mice after an i.p. injection of CaMKII inhibitor KN-93 (10–30 μmol/kg) (19). Injection of KN-93 reduced the incidence of AF episodes to 13% in *Ryr2*^{R176Q/+} mice (*P* < 0.05 compared with untreated mice) (Figure 3, A and E). In contrast, the inactive analog KN-92 did not prevent pacing-induced episodes of AF in *Ryr2*^{R176Q/+} mice (Figure 3C). Baseline electrophysiological parameters were unaltered in both *Ryr2*^{R176Q/+} and WT mice 10 minutes after injection of KN-93 (Supplemental Table 2). Similarly, the electrical properties of the conduction system, as measured by sinus node recovery time, AERP, and atrioventricular nodal effective refractory period, were not different between *Ryr2*^{R176Q/+} and WT mice after KN-93 administration (Supplemental Table 2).

We next sought to confirm these pharmacological studies in transgenic mice expressing the CaMKII inhibitory protein AC3-I in the heart (20). Expression of AC3-I reduces cardiac CaMKII activity by about 50% (20). In contrast, mice expressing the scrambled AC3-C peptide in the heart have normal CaMKII activity (20). WT and *Ryr2*^{R176Q/+} mice were interbred with AC3-I and AC3-C transgenic mice, respectively. Inducibility of AF was determined using the rapid atrial pacing protocol. *Ryr2*^{R176Q/+} mice overexpressing the AC3-I peptide in the heart exhibited a significantly lower incidence of pacing-induced AF (16%) compared with *Ryr2*^{R176Q/+} mice (*P* < 0.05) (Figure 3, B and E). In contrast, *Ryr2*^{R176Q/+} mice crossed with transgenic mice expressing the inactive peptide analog AC3-C had AF incidence similar to that of *Ryr2*^{R176Q/+} mice (62%; Figure 3, D and E). The average duration of AF in the *Ryr2*^{R176Q/+}.AC3-C mice was 8.7 ± 3.3 seconds, which showed a tendency to be longer than the 3.4-second episode recorded in the only *Ryr2*^{R176Q/+}.AC3-I mouse exhibiting an AF episode (*P* = NS).

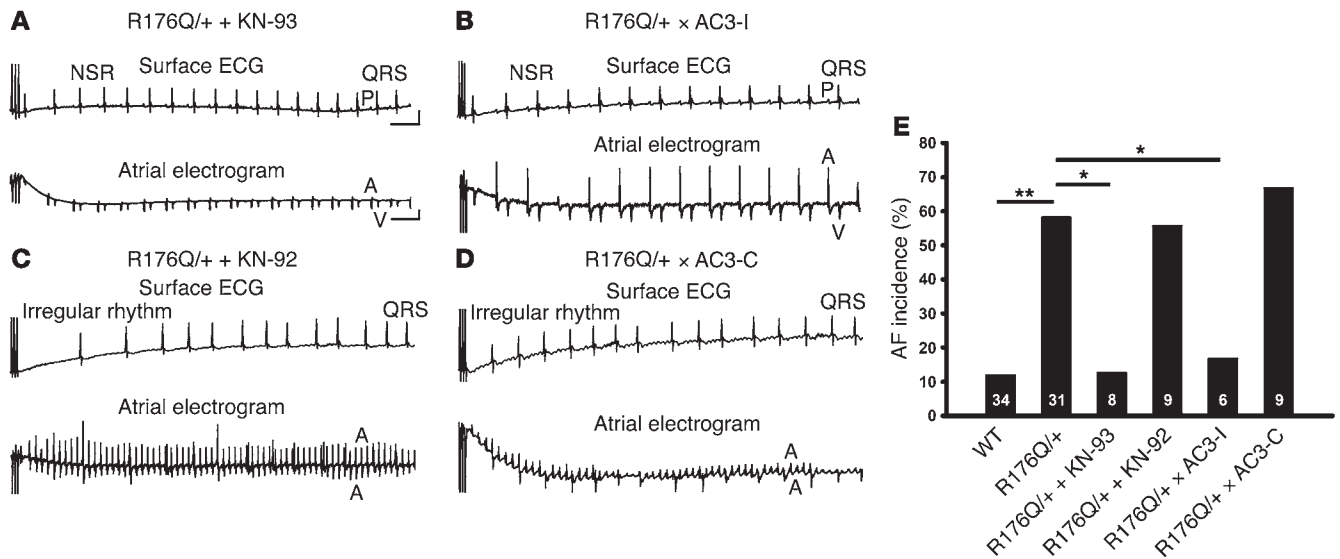


Figure 3

Pharmacological and genetic inhibition of CaMKII prevents pacing-induced AF in *Ryr2*^{R176Q/+} knockin mice. (A) Surface ECG and intracardiac atrial electrogram showing prevention of pacing-induced AF in *Ryr2*^{R176Q/+} mice treated with CaMKII inhibitor KN-93. Scale bar: 0.1 mV (vertical axis); 100 ms (horizontal axis). (B) Surface ECG and intracardiac atrial electrogram showing prevention of pacing-induced AF in *Ryr2*^{R176Q/+} knockin mice expressing the CaMKII peptide inhibitor AC3-I. (C) Surface ECG and intracardiac atrial electrogram showing pacing-induced AF in *Ryr2*^{R176Q/+} knockin mice treated with the KN-93 inactive analog KN-92. (D) Surface ECG and intracardiac atrial electrogram showing pacing-induced AF in *Ryr2*^{R176Q/+} mice expressing the AC3-I inactive peptide analog AC3-C. (E) Bar graph summarizing percentages of mice in which AF could be induced using rapid pacing. Numbers in bars indicate numbers of mice tested in each group. **P* < 0.05; ***P* < 0.001.

Absence of atrial remodeling and normal levels of Ca²⁺-handling proteins in atria of Ryr2^{R176Q/+} mice. Atrial enlargement and fibrosis are important predisposing factors for the development of AF in patients. Examination of longitudinal heart sections from *Ryr2*^{R176Q/+} and WT mice stained with H&E, however, revealed normal atrial size and microscopic structure (Supplemental Figure 4, A and B). There were no significant differences comparing *Ryr2*^{R176Q/+} and WT mice in the longitudinal (1.61 ± 0.04 vs. 1.62 ± 0.05 mm) or transverse (0.58 ± 0.02 vs. 0.60 ± 0.03 mm) diameters of the left atria. Similarly, there were no differences in right atrial diameters (data not shown). Masson trichrome staining demonstrated the absence of interstitial fibrosis in both groups (Supplemental Figure 4, C and D). Moreover, ventricular dimensions are similar in *Ryr2*^{R176Q/+} and WT mice, as previously reported (15, 20).

We also examined the possibility that the R176Q mutation in the *Ryr2* gene could trigger compensatory changes in other Ca²⁺-handling proteins, which might be responsible for an increased AF susceptibility. RT-PCR did not reveal any significant differences in the mRNA (Supplemental Figure 5, A and B) expression levels of RyR2, the α subunit of the L-type voltage gated Ca²⁺ channel (Cav1.2), Na⁺/Ca²⁺ exchanger (NCX1), SERCA2a, and PLN in the atria of *Ryr2*^{R176Q/+} and WT mice (Supplemental Figure 5, A and B). Western blot analysis of the same Ca²⁺-handling proteins also showed unaltered protein expression levels in *Ryr2*^{R176Q/+} mice (Supplemental Figure 5, C and D). Taken together, these findings strongly suggest that the phenotypic difference in atrial electrophysiology observed in *Ryr2*^{R176Q/+} mice is the direct consequence of the R176Q mutation in RyR2 and is not due to compensatory changes in expression levels of other key Ca²⁺-handling proteins.

Elevated SR Ca²⁺ leak in atrial myocytes from Ryr2^{R176Q/+} mice. We have previously demonstrated that genetic mutations in *Ryr2* may

cause diastolic SR Ca²⁺ leak and ventricular arrhythmias (15, 21). Here, we examined the hypothesis that the R176Q mutation in *Ryr2* may confer increased leakiness of the atrial RyR2 Ca²⁺ channel. Enzymatically isolated single atrial myocytes were loaded with a Ca²⁺-sensitive dye and subjected to electrical field stimulation. The amplitude of the evoked Ca²⁺ transients was comparable for *Ryr2*^{R176Q/+} and WT mice (in AU of fluorescence: 1.96 ± 0.13 [*n* = 46] vs. 1.72 ± 0.14 [*n* = 44]; *P* = NS) (Figure 4, A and B). However, the magnitude of SR Ca²⁺ leak, measured using the protocol described by Shannon et al. (22), was significantly larger in *Ryr2*^{R176Q/+} atrial myocytes (0.56 ± 0.08 AU of fluorescence) compared with WT atrial myocytes (0.25 ± 0.03 AU; *P* < 0.05) (Figure 4, A and B). The SR Ca²⁺ content estimated by rapid application of 10 mM caffeine was similar in *Ryr2*^{R176Q/+} myocytes (4.59 ± 0.42 AU) compared with WT mice (4.04 ± 0.41 AU; *P* = NS). Thus, under conditions of comparable SR Ca²⁺ loads, SR Ca²⁺ leak was significantly higher in *Ryr2*^{R176Q/+} (10.2% ± 0.9%) compared with WT atrial myocytes (7.7% ± 0.8%; *P* < 0.05; Figure 4C). Similar experiments were performed in the presence of CaMKII inhibitor KN-93 (1 μ Mol/l). The enhancement of SR Ca²⁺ leak in *Ryr2*^{R176Q/+} atrial myocytes was reversed by CaMKII inhibition to levels observed in WT myocytes after CaMKII inhibition (Figure 4C).

Ectopic activity and reentry in paced atria from Ryr2^{R176Q/+} mice. The main electrophysiological mechanisms proposed to underlie AF are reentry (23) and ectopic activity (24, 25). We examined the hypothesis that mutations in *Ryr2* increase the predisposition of *Ryr2*^{R176Q/+} mouse atria to ectopic activity and reentry. Under control conditions during pacing at 5 Hz, the atrial action potential duration at 80% repolarization (APD₈₀) averaged 24 ± 1 ms in WT (*n* = 4) vs. 23 ± 1 ms in *Ryr2*^{R176Q/+} mice (*n* = 5) (*P* = NS), whereas the APD₅₀ was 13.2 ± 0.5 ms in WT and 13.2 ± 0.5 ms in *Ryr2*^{R176Q/+} mice

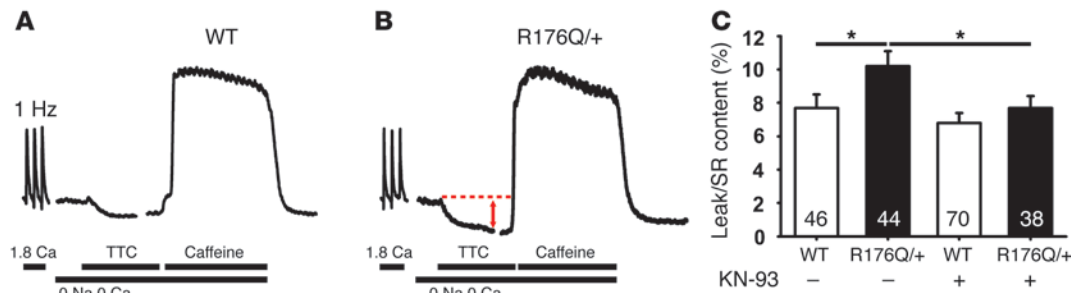


Figure 4

Pharmacological inhibition of CaMKII reverses enhanced SR Ca²⁺ leak in *Ryr2^{R176Q/+}* atrial myocytes. Representative [Ca²⁺]_i recordings obtained from fluo-4 AM-loaded atrial myocytes from WT (A) and *Ryr2^{R176Q/+}* (B) mice during 1 Hz pacing in 1.8 mM Ca²⁺ (left), followed by a rapid switch to Tyrode solution containing 0 Na⁺, 0 Ca²⁺, and tetracaine (TTC) (1 mmol/l). Tetracaine was washed out 30 seconds later, and SR Ca²⁺ content was measured by changing superfusate to 10 mmol/l caffeine in 0 Na⁺, 0 Ca²⁺ Tyrode solution. SR Ca²⁺ leak was measured as shown in red and related to SR Ca²⁺ content. (C) Bar graph represents quantification of SR Ca²⁺ leak normalized to SR Ca²⁺ content in the presence and absence of KN-93 in WT and *Ryr2^{R176Q/+}* atrial myocytes. **P* < 0.05. Numbers in bars indicate numbers of myocytes tested.

(*P* = NS). Similarly, the intracellular Ca²⁺ transient [Ca²⁺]_i duration averaged 113 ± 5 ms in WT vs. 107 ± 4 ms in *Ryr2^{R176Q/+}* mice (*P* = NS). Conduction velocities at a BCL of 200 ms were (in mm/ms) 0.34 ± 0.16 in WT and 0.39 ± 0.13 in *Ryr2^{R176Q/+}* mice (*P* = NS).

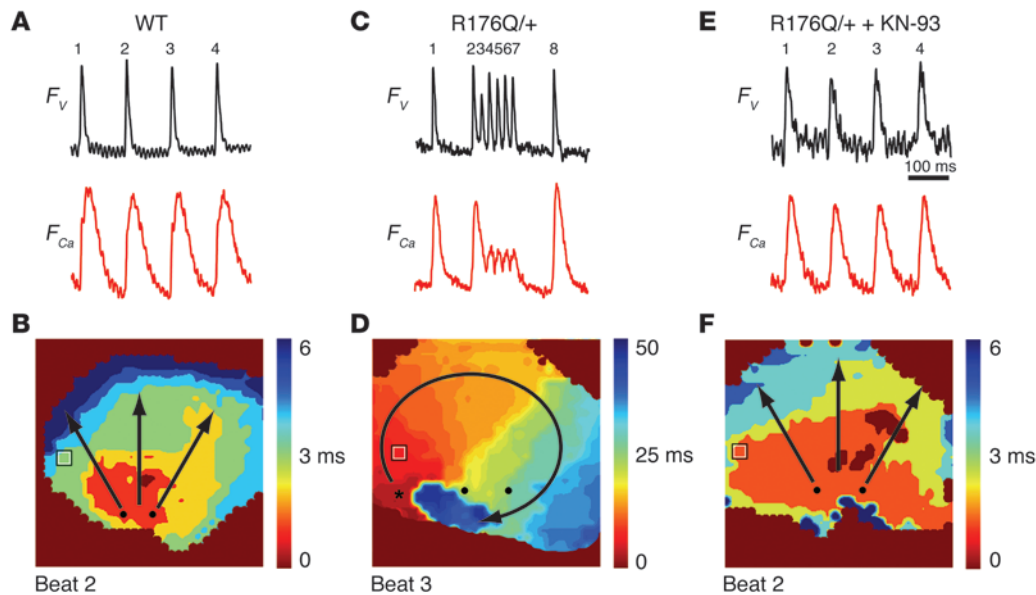
Atrial pacing using an atrial burst protocol similar to that used in the in vivo studies led to 1:1 capture by WT (*n* = 4) and *Ryr2^{R176Q/+}* (*n* = 5) atria (Figure 5, A and B). Atrial pacing induced more frequent ectopic beats in *Ryr2^{R176Q/+}* (262 of 1770 beats were ectopic in a total of 5 preparations, using 2 pacing protocols) than in WT (19 of 1416 beats were ectopic in 4 preparations, using 2 pacing protocols) atria (*P* < 0.001 using χ^2). Ectopic beats in *Ryr2^{R176Q/+}* atria occurred at a pacing cycle length (CL) between 180 and 120 ms, while in WT atria, they occurred at a much faster pacing CL of 120 ms. Ectopic beats occurred spontaneously, arising during the decay of the preceding (paced) Ca²⁺ transient. The sites of ectopic beat initiation were not consistent in any given tissue, and locations would vary in different episodes. Ectopic beats initiated reentry in 3 of 5 *Ryr2^{R176Q/+}* atria, as illustrated by the rotating activation pattern of electrical propagation, with the latest activating sites localized adjacent to the earliest activation sites of consecutive beats (Figure 5, C and D). The dynamics of the reentry circuit are even more evident in Supplemental Figure 6 and Supplemental Video 1, where ectopic beat 3 from Figure 5C induces several consecutive reentrant electrical waves (Supplemental Video 1). Incubation of atria with 1 μ mol/l KN-93 suppressed ectopic activity and reentry in all *Ryr2^{R176Q/+}* atria that showed this behavior prior to incubation (Figure 5, E and F).

Increased CaMKII-dependent phosphorylation of RyR2 in atria of patients with chronic AF and goats with lone AF. To determine the potential implications of our findings for clinical AF, we assessed the level of CaMKII activation and CaMKII-dependent phosphorylation of RyR2 in atrial biopsies obtained from patients in chronic AF who underwent coronary artery bypass graft surgery. The clinical characteristics of the patients with and without AF are summarized in Supplemental Table 3. There were no significant differences between the groups relative to age, LV ejection fraction, LV end-diastolic pressure, or left atrial end-diastolic diameter, which excluded significant differences in the degree of structural heart disease. Phosphorylation of RyR2 at S2814 was increased by approximately 60% in patients with chronic AF compared with patients in sinus rhythm (Figure 6A). Levels of total and T287-autophosphorylated CaMKII were 63% and 40% higher in patients

with chronic AF compared with sinus rhythm patients, respectively (Figure 6B). Consistent with prior studies (4), phosphorylation of RyR2 at S2808 was also increased in patients with chronic AF (Supplemental Figure 7).

To determine the specific effect of AF on CaMKII activity and CaMKII phosphorylation in the absence of structural heart disease, we analyzed atrial samples from the well-characterized goat model of sustained (lone) AF. Sustained AF was induced by repetitive burst pacing using an automatic pacemaker (26). At the time of tissue collection, goats were in sustained AF for 7 to 10 days but had preserved atrial dimensions and no atrial fibrosis (data not shown). Western blot analysis revealed that CaMKII phosphorylation of S2814 on RyR2 was significantly elevated in goats with lone AF compared with control goats in sinus rhythm despite the absence of structural heart disease (Figure 6, C and D), confirming previous findings (27). Moreover, the higher CaMKII phosphorylation of S2814 on RyR2 was consistent with an increase of CaMKII autophosphorylation at T287, pointing to enhanced CaMKII activity as the potential underlying mechanism of increased RyR2 phosphorylation in AF goats. As shown recently (27), PKA phosphorylation of RyR2 at S2808 was not changed in the atria of goats with lone AF (Supplemental Figure 7). These data suggest that – at least in the goat – the increase in CaMKII activity and the subsequent CaMKII phosphorylation of RyR2 precede the development of structural heart disease and atrial fibrosis, similar to the concept that CaMKII-mediated RyR2 leak in ventricular myocardium from mice with CaMKII overexpression precedes ventricular remodeling and sudden death (28), pointing to a potential role of CaMKII signaling in early atrial remodeling and eventually in the progression to chronic atrial disease.

Increased CaMKII-dependent phosphorylation of RyR2 in atria from CREM-Ib Δ C-X-overexpressing mice. We further tested the contribution of CaMKII to RyR2 phosphorylation in a mouse model with spontaneous AF development in the context of structural heart disease. Whereas about a dozen mouse models of AF have been described, few transgenic mouse strains actually exhibit spontaneous AF in the presence of structural remodeling in the atria. Mice with cardiac-specific overexpression of CREM-Ib Δ C-X, a member of the transcription factor family of cAMP-response element-binding proteins (CREB)/CREM, show atrial dilatation at an age of 8 weeks associated with the development of persistent AF and a rapid

**Figure 5**

Pacing-induced ectopic activity and reentry in *Ryr2^{R176Q/+}* mouse atria is suppressed by pharmacological inhibition of CaMKII. (A) Simultaneous recordings of voltage (F_v) and Ca^{2+} fluorescence (F_{Ca}) traces in WT mouse atria at pacing CL of 140 ms. (B) Voltage isochronal map corresponding to the paced beat 2 showing wavefront propagation across the atria (arrows) starting from the pacing electrode at the bottom (black dots). (C) Simultaneous recordings of F_v and F_{Ca} traces in *Ryr2^{R176Q/+}* mouse atria at pacing CL of 140 ms demonstrating an ectopic beat occurring during the decline of the Ca^{2+} transient corresponding to beat 2, which initiates reentry. (D) Voltage isochronal map corresponding to the ectopic beat (beat 3) showing a circular propagation pattern across the atria (arrow) consistent with a reentrant circuit. The origin of the ectopic beat is indicated by an asterisk, and the circular propagation is indicated by the circular arrow. Black dots represent the position of the pacing electrodes. (E) Simultaneous recordings of F_v and F_{Ca} traces in *Ryr2^{R176Q/+}* mouse atria from D after incubation with the CaMKII inhibitor KN-93. CaMKII inhibition suppresses ectopic activity and reentry at pacing CL of 140 ms. (F) Isochronal map corresponding to beat 2 shows propagation pattern across the atria from pacing electrode at the bottom (black dots). Ectopic beats and reentry were suppressed by CaMKII inhibition. Squares in B, D, and F represent the pixel at which the voltage and Ca^{2+} signals were sampled in A, C, and E, respectively.

ventricular response beginning at weeks 16–20 (29). Western blot analysis of flash-frozen whole atria from CREM-IbΔC-X transgenic mice and age-matched controls revealed increased PKA phosphorylation of RyR2 at S2808 (Supplemental Figure 7) and enhanced CaMKII phosphorylation of RyR2 at S2814 in CREM-IbΔC-X transgenic mouse atria compared with WT mice (Figure 7). Because increased CaMKII phosphorylation of S2814 was a consistent finding among all animal models of AF studied, our findings provide additional evidence for the importance of CaMKII signaling and RyR2 dysfunction in the evolution of AF.

Genetic inhibition of S2814 phosphorylation on RyR2 prevents AF induction. To determine whether CaMKII phosphorylation of RyR2 is a critical downstream target of CaMKII involved in the induction of AF, we generated knockin mice in which S2814 on RyR2 was substituted by alanine (S2814A) (Figure 8, A–F). The *Ryr2^{S2814A}* knockin mice were born at rates consistent with a Mendelian inheritance pattern. In WT mouse heart, CaMKII was able to phosphorylate RyR2 and CaMKII inhibitor KN-93 prevented this phosphorylation event (Figure 8G). CaMKII phosphorylation of RyR2 was mostly inhibited in *Ryr2^{S2814A}* homozygous knockin mice, suggesting that S2814 is the major CaMKII phosphorylation site on RyR2. During baseline ECG recordings, none of the *Ryr2^{S2814A}* knockin or WT mice developed spontaneous AF, and baseline heart rates were similar in both genotypes (WT: 564 ± 12 bpm; *Ryr2^{S2814A}*: 551 ± 12 bpm). Because our previous studies suggested that AF can only be induced and maintained in the presence of a suitable substrate, we used the vagotonic AF model previously described by Berul et al. (30)

to determine the specific role of the RyR2-S2814 phosphorylation site for AF induction. AERPs were not different, comparing WT and *Ryr2^{S2814A}* mice in the absence (WT: 46.3 ± 0.7 ms; *Ryr2^{S2814A}*: 47.4 ± 1.7 ms) or presence of carbachol (WT: 45.2 ± 0.4 ms; *Ryr2^{S2814A}*: 47.7 ± 1.5 ms), suggesting there were no differences in the underlying arrhythmogenic substrate induced by the S2814A mutation in RyR2. Whereas rapid atrial pacing could induce AF in 44% of WT mice (7 of 16), *Ryr2^{S2814A}* knockin mice were more resistant to pacing-induced AF in the presence of cholinergic stimulation with carbachol (7.7%, 1 of 13; $P < 0.05$) (Figure 8H). These findings suggest that in the presence of an arrhythmogenic substrate (i.e., cholinergic stimulation), rapid atrial pacing-induced CaMKII phosphorylation of S2814 on RyR2 is the critical event supporting AF induction in mice.

Discussion

Abnormal SR Ca^{2+} release in chronic AF. It is generally accepted that atrial remodeling in chronic AF leads to abnormalities of intracellular Ca^{2+} cycling during excitation-contraction coupling. Furthermore, it has been hypothesized that these defects in Ca^{2+} homeostasis may contribute to the arrhythmogenic substrate that sustains AF (3, 4, 31). In human atrial myocytes obtained from patients in paroxysmal or chronic AF, an increased number of spontaneous Ca^{2+} releases from the SR were detected (3), with spontaneous Ca^{2+} spark frequency being higher in AF patients than in patients in sinus rhythm (3). The amplitude of the L-type voltage-gated Ca^{2+} current is typically decreased in AF (5, 6), which has led us and others to speculate that

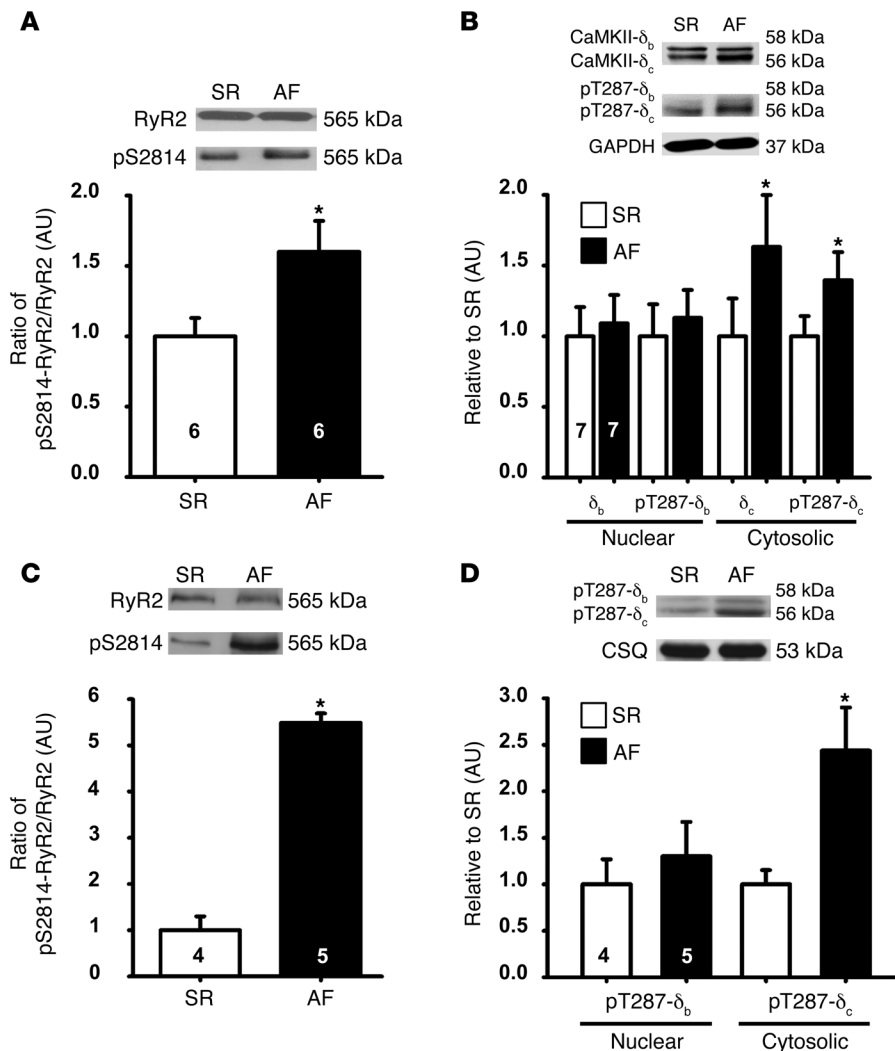


Figure 6

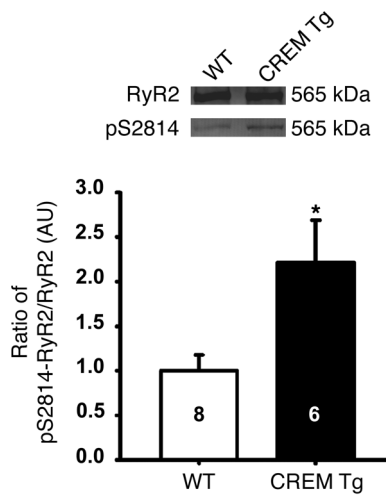
Increased CaMKII-dependent phosphorylation of RyR2 at S2814 in atria of patients with chronic AF and goats with lone AF. (A) Examples of RyR2 and phosphorylated RyR2-S2814 in atria of patients in sinus rhythm (SR) and chronic AF. Bottom: mean ± SEM protein-band intensities phosphorylated RyR2-S2814 relative to total RyR2 (*n* = 6 for SR and *n* = 6 for AF atria/analysis; **P* < 0.05 versus SR). Numbers in bars indicate numbers of atria used per group. (B) Examples of total CaMKII δ , CaMKII-pT287 (autophosphorylated), and GAPDH immunoblots. Top bands (58 kDa) represent nuclear CaMKII δ_b and bottom (56 kDa) cytosolic CaMKII δ_c isoforms. Bottom: mean ± SEM protein-band intensities normalized to GAPDH, expressed relative to SR (*n* = 7 for SR and *n* = 7 for AF; **P* < 0.05 versus SR). (C) Examples of RyR2 and phosphorylated RyR2-S2814 in atria of goats in SR and AF. Bottom: mean ± SEM protein-band intensities phosphorylated RyR2-S2814 relative to total RyR2 (*n* = 4 for SR and *n* = 5 for AF; **P* < 0.05 versus SR). (D) Examples of total CaMKII-pT287 (autophosphorylated) and calsequestrin (CSQ) immunoblots. Top bands (58 kDa) represent pT287-CaMKII δ_b and bottom (56 kDa) pT287-CaMKII δ_c . Bottom: mean ± SEM protein-band intensities normalized to CSQ, expressed relative to ST (*n* = 4 SR and *n* = 5 AF; **P* < 0.05 versus SR).

abnormal Ca²⁺ release events in AF might be caused by enhanced activity of RyR2 Ca²⁺ release channels (4, 7). This could promote diastolic SR Ca²⁺ release and Ca²⁺ wave generation that may cause delayed afterdepolarizations and create an arrhythmogenic substrate favoring AF initiation or maintenance (9, 32). Using single-channel bilayer recordings, Vest et al. demonstrated an increased open probability of RyR2 channels isolated from dogs in persistent AF (4). This finding and the observation that RyR2 expression levels are unaltered or decreased in patients with chronic AF (33–36) suggest that remodeling of the RyR2 macromolecular complex may underlie the defective channel function in chronic AF.

To gain more insight into the specific contribution of abnormal RyR2 activity in atrial arrhythmogenesis, we chose as a model mice carrying a gain-of-function mutation R176Q in RyR2. This mutation was previously identified in patients with ventricular arrhythmias caused by leaky RyR2 channels (14, 16). We were initially surprised to find that *Ryrr2*^{R176Q/+} mice do not develop spontaneous AF when monitored with telemetry. Our data suggest that a gain-of-function RyR2 defect alone is not sufficient to produce enhanced propensity to arrhythmias. Similar observations were made by Venetucci et al. (11) in isolated rat ventricular myocytes. Using caffeine, isoproterenol, or a combination of both compounds, it was

shown that simply increasing open probability of normal RyR2 channels is not sufficient to produce arrhythmogenic diastolic Ca²⁺ release (11). In contrast, we found that rapid atrial pacing was an effective trigger for increasing CaMKII, amplifying SR Ca²⁺ leak, and generating Ca²⁺-induced afterdepolarizations and AF. Thus, the gain-of-function mutation in RyR2 of *Ryrr2*^{R176Q/+} mice (AF-promoting substrate) requires a triggering event (rapid atrial pacing with subsequent activation of CaMKII) to induce AF episodes (“double-hit concept”).

Some clinical studies are consistent with our findings that gain-of-function defects in RyR2 create a substrate for the development of AF. Sumitomo et al. (37) demonstrated an increased AF incidence in a patient with a genetic mutation in the *Ryrr2* gene, associated with catecholaminergic polymorphic ventricular tachycardia. This patient did not develop spontaneous AF, but episodes of AF could be induced by isoproterenol infusion or atrial pacing (37). These clinical observations support the dual requirement for atrial arrhythmogenesis of a predisposing RyR2 defect and rapid atrial pacing causing abnormal activation of CaMKII, which is consistent with our observations in mice with a gain-of-function mutation in RyR2. Pizzale et al. (38) also reported evidence for AF in a 19-year-old patient with catecholaminergic polymorphic ventricular tachy-



cardia due to a missense mutation in *Ryr2*. In a third study, Bhuiyan et al. (39) showed that members of 2 families with an exon 3 defect in the *Ryr2* gene also had abnormalities in sinoatrial node function as well as atrioventricular nodal function, atrial standstill, and AF (39). Whereas a genetic form of RyR2-mediated AF is likely to be very rare, these observations do suggest that abnormal intracellular Ca^{2+} release may – under certain circumstances – promote atrial arrhythmogenesis in otherwise healthy individuals (39).

Dual requirement for an arrhythmogenic substrate and a triggering event involving CaMKII in AF induction. Our data suggest that, under conditions that activate CaMKII in the atria, amplification of the gain-of-function defect in RyR2 and subsequent diastolic SR Ca^{2+} leak enhance the susceptibility to pacing-induced AF in *Ryr2*^{R176Q/+} mice. The observation that both pharmacological and genetic inhibition of CaMKII reduce the vulnerability to pacing-induced AF supports this model. Activated CaMKII is likely to phosphorylate multiple downstream targets in cardiomyocytes, including RyR2, PLN, L-type Ca^{2+} channels, and Na^+ channels. Because the pacing-induced increase in CaMKII phosphorylation of both RyR2 and PLN was equal for *Ryr2*^{R176Q/+} and WT mice but only *Ryr2*^{R176Q/+} mice were susceptible to pacing-induced AF, the most likely explanation for the pronounced difference in the incidence of pacing-induced AF in *Ryr2*^{R176Q/+} mice is the single amino acid mutation in RyR2 that provides the arrhythmogenic substrate in this model. Because the mutation by itself, however, is not sufficient to initiate spontaneous AF, CaMKII most likely amplifies SR Ca^{2+} leak, thus promoting atrial arrhythmogenesis in this model. Of course, it is important to note that SR Ca^{2+} leak may be enhanced directly (due to a further increase in RyR2 open probability after CaMKII phosphorylation) (18, 40) and/or indirectly (due to increased SR Ca^{2+} reuptake, as a result of increased PLN phosphorylation with subsequent increase in SERCA2a function, among other things) (41). Other data obtained in atrial biopsies from patients with chronic AF, goats with lone AF, and mice with spontaneous AF are in agreement with the double-hit concept, in which 2 factors are required for AF induction: (a) a tissue or cellular abnormality (AF-maintaining substrate) that can be a genetic mutation (for instance, in RyR2) or atrial remodeling (electrical or structural) and (b) a triggering event (for instance, abnormal activation of CaMKII).

Increased expression levels of CaMKII have been reported in patients with chronic AF (42). Consistent with these findings,

Figure 7

Increased CaMKII-dependent phosphorylation of RyR2 at S2814 in atria of CREM-Ib Δ C-X transgenic mice. Top: representative examples of RyR2 and phosphorylated RyR2-S2814 in atria of CREM-Ib Δ C-X transgenic and WT mice. Bottom: mean values \pm SEM of protein-band intensities of phosphorylated RyR2-S2814 relative to total RyR2 ($n = 8$ for WT and $n = 6$ for CREM Tg “atria/analysis”; * $P < 0.05$). Numbers in bars indicate numbers of atria tested.

CaMKII-dependent phosphorylation of PLN (residue T17) was higher in right-atrial appendages of patients in chronic AF than in sinus rhythm patients (31). Elevated PLN phosphorylation occurred despite higher total activity of type 1 (PP1) and type 2A phosphatases in chronic AF (31), suggesting local differences in protein phosphatase activity within different microdomains in atrial myocytes during AF. Our findings extend these observations to the RyR2 channel complex, as phosphorylation of RyR2 at S2814 was increased in patients with chronic AF (Figure 6). We have previously shown that CaMKII binds to the RyR2 macromolecular complex (18, 43, 44) and S2814 is the main CaMKII site on RyR2 (18). In the present study, we found that the expression level and autophosphorylation of the cytosolic CaMKII δ isoform is increased in patients with chronic AF, suggesting that hyperphosphorylation of RyR2 at S2814 likely results from higher CaMKII expression and activity levels. Whereas electrical and structural remodeling are strong determinants of the arrhythmogenic substrate in patients with chronic AF (12, 45), increased CaMKII activity and, in particular, CaMKII hyperphosphorylated RyR2 may contribute to the initiation and/or perpetuation of AF. Our data obtained in goats with lone AF with no evidence of structural heart disease, showing enhanced CaMKII phosphorylation of RyR2-S2814, suggest that – at least in the goat – the increase in CaMKII activity and the subsequent CaMKII phosphorylation of RyR2 precede the development of structural heart disease and atrial fibrosis, pointing to a potential role of CaMKII signaling in early atrial remodeling and eventually in the progression of the arrhythmia to a chronic state.

Consistent with previous studies by Vest et al. (4), we found that atrial RyR2 from patients with chronic AF is hyperphosphorylated at S2808. Therefore, it is possible that increased PKA phosphorylation of S2808 may contribute to defective SR Ca^{2+} release events in AF patients (3). Our findings that phosphorylation of S2808 on RyR2 was not elevated in *Ryr2*^{R176Q/+} mice or goats with lone AF, however, suggests that AF can be induced and maintained in these models in the absence of hyperphosphorylation of S2808. On the other hand, PKA phosphorylation of S2808 was increased not only in AF patients but also in CREM-Ib Δ C-X transgenic mice, suggesting that PKA hyperphosphorylation of RyR2 at S2808 may be associated with AF in the structurally remodeled atria, potentially contributing to AF maintenance.

Abnormal SR Ca^{2+} release, ectopic activity, and reentry in AF. Three major mechanisms have been proposed to explain the initiation and maintenance of AF: ectopic activity, a single circuit reentry, or mother rotor and multiple circuit reentry (46). AF can be initiated or sustained by bursts of premature excitations originating primarily in the pulmonary veins (PVs) (24, 25). Several studies point to the importance of abnormal Ca^{2+} regulation as trigger and substrate for PV arrhythmogenic activity (47–49). Application of the RyR2 inhibitor ryanodine inhibited PV firing, suggesting the requirements of RyR2-mediated Ca^{2+} release in arrhyth-

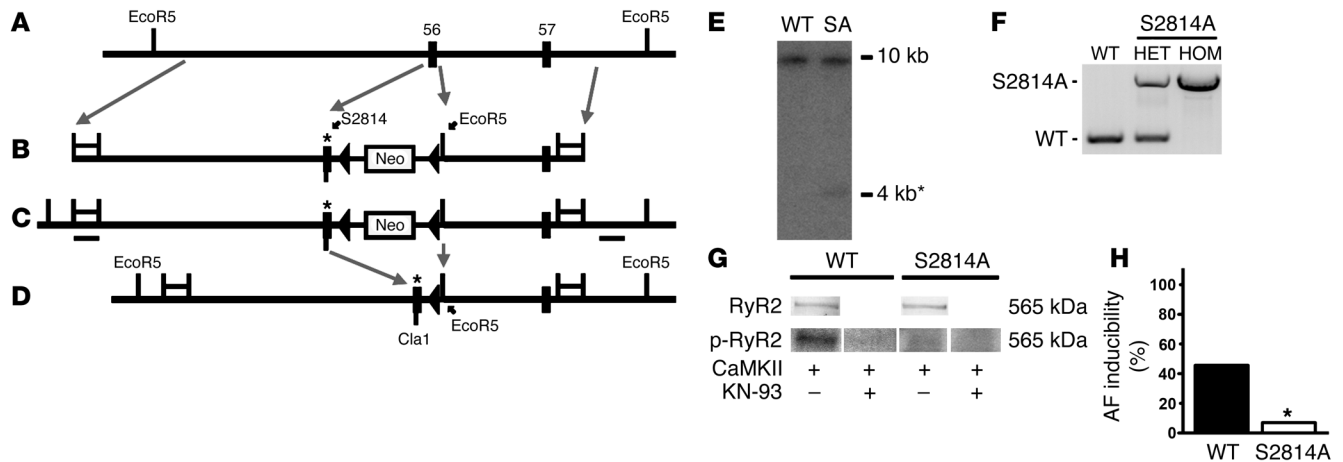


Figure 8 Mutation S2814A in RyR2 prevents AF in *Ryr2^{S2814A}* knockin mice. (A) Targeted engineering of the S-to-A mutation of S2814 in the mouse RyR2 locus. A genomic clone containing exons 56 and 57 of the mouse *Ryr2* gene was isolated from a 129/SvJ λKO-1 library and cloned into a pDTA4B vector using homologous recombination. (B) The S2814A mutation was introduced into exon 56 of RyR2 along with a new ClaI site. A cassette containing a loxP-flanked *NeoR* gene expressed from the phosphoglycerate kinase promoter (PGK-*NeoR*) was cloned into intron 56 to obtain the final targeting vector. (C) Targeting vector was linearized with *Pme1* and electroporated into AB2.2 129Sv/J ES cells. Homologous-targeted integrands were identified using Southern blot analysis. (D) Following germline transmission and crossing with *Meox2-Cre* mice, final allele without *Neo* cassette was obtained. (E) Southern blot analysis reveals homologous-targeted mutant allele (*). (F) Heterozygous mice (HET) are bred to obtain homozygous knockin mice (HOM), identified by PCR genotyping. (G) Autoradiograph showing that CaMKII phosphorylation in the presence of γ -ATP³² was greatly inhibited in RyR2 from S2814A mouse heart. Immunoprecipitated RyR2 (input) is shown (top). Half the sample was CaMKII phosphorylated in the presence or absence of KN-93 (bottom). Noncontiguous lanes are separated by white lines. (H) Electrophysiology studies revealed that AF could be induced by cardiac pacing in 44% of WT mice after carbachol injection (50 ng/g body weight i.p.) compared with 7.7% of *Ryr2^{S2814A}* mice (**P* < 0.05).

mia formation (49). Stabilization of RyR2 with the experimental compound K201 (JTV519) reduces the arrhythmogenic activity of PV cardiomyocytes (50). Arrhythmogenic activity due to ectopic activity does not exclusively originate from PVs but can arise from atrial sites outside the PVs (51). Our data revealed that rapid atrial pacing caused ectopic activity in *Ryr2^{R176Q/+}* more frequently than in WT atria. Moreover, ectopic activity occurred at longer pacing CLs in *Ryr2^{R176Q/+}* compared with WT atria, whereas inhibition of CaMKII with KN-93 resulted in suppression of ectopic activity in *Ryr2^{R176Q/+}* atria. Interestingly, ectopic activity arose during the decay of a paced Ca²⁺ transient, suggesting early rather than delayed afterdepolarizations as the potential underlying mechanism. Similar afterdepolarizations arising during late phase 3 of the action potential have been implicated in the initiation of AF (52) and in other models of Ca²⁺ overload such as ischemia (53, 54). It is presumed that this mechanism involves an increase in [Ca²⁺]_i during the final phase of repolarization at voltages negative to the equilibrium potential for NCX and that this combination of changes leads to increased inward NCX current that generates early afterdepolarizations and triggered activity (55).

Ectopic activity and reentry can interact with each other and promote AF maintenance. In *Ryr2^{R176Q/+}* atria, we demonstrated ectopic beats leading to reentry and self-sustained wave propagations, which could lead to AF in whole heart. This pattern was not observed after CaMKII inhibition with KN-93, as the ectopic activity was suppressed. The fact that reentrant circuits were not exactly identical, with beat-to-beat variations and mild reentry meandering, supports a fibrillatory pattern rather than a regular tachycardia. Our model was not designed to solve controversies about the proposed AF mechanisms. However, we do show that a single molecular altera-

tion leads to a phenotype that replicates ectopic activity and reentry, as has been shown in large animal models of AF (56).

Nevertheless, optical mapping studies in dogs with rapid atrial tachycardia and in goats with sustained (lone) AF do not provide clear evidence for focal atrial discharges (12) and suggest reentry as the main mechanism maintaining AF in these models. In patients with long-term AF and accompanying heart diseases, it is quite possible that the combined influences of atrial tachycardia and heart disease-based remodeling perturb atrial Ca²⁺ handling to produce Ca²⁺-induced triggered activity and focal sources driving AF. Thus, although Ca²⁺-dependent focal sources are often suggested as playing a critical role in the pathogenesis of AF, direct experimental proof of the relationship between local Ca²⁺ release events and focal activity in fibrillating atria is lacking in patients, most likely because of limitations of currently used mapping systems to clearly discriminate between reentry and focal activity. Further refinement of high-resolution mapping systems for simultaneous endo-epicardial recordings in combination with improved bioinformatics tools is needed to develop reliable discrimination criteria of reentry and focal activity.

Proarrhythmic effect of CaMKII hyperphosphorylation of RyR2 at S2814. To determine the potential proarrhythmic role of CaMKII phosphorylation of RyR2 as a specific downstream target of activated CaMKII, we generated and studied *Ryr2^{S2814A}* knockin mice, in which RyR2 phosphorylation by CaMKII was impaired. We used a vagotonic model of AF (30), in which acute cholinergic stimulation associated with a shortening of the AERP was used to produce a substrate for AF in the structurally normal mouse heart. Following carbachol injection, AF could be induced by rapid atrial pacing in about half of the WT mice, whereas most *Ryr2^{S2814A}* knockin



mice were resistant to pacing-induced AF. These findings provide direct and specific evidence that RyR2 is a target of CaMKII required for AF inducibility in this mouse model. Although other downstream targets of CaMKII (e.g., PLN, Cav1.2, Nav1.5) may also contribute, based on the findings obtained in *Ryr2^{S2814A}* knockin mice, we propose that phosphorylation of RyR2 at S2814 is a critical, albeit not necessarily exclusive, downstream target of CaMKII in AF development.

Study limitations. It is possible that the effects of CaMKII-dependent phosphorylation of defective RyR2 in human atria and especially in diseased hearts are different than those in mice and of lesser importance in promoting an arrhythmogenic substrate for AF initiation and maintenance. For example, it is conceivable that relatively small SR Ca²⁺ release events might be sufficient to induce afterdepolarizations in mice due to the faster repolarization phase, whereas in larger animals and humans with longer action potentials, greater SR Ca²⁺ leaks might be necessary to cause triggered activity. However, we performed extensive validation studies to dissect the specific influences of AF on CaMKII phosphorylation of RyR2 in the absence (goats) and presence of structural heart disease (CREM-IbAC-X transgenic mice). Consistent with the principal findings in patients with chronic AF, we found increased CaMKII activity and CaMKII phosphorylation in both models. Nevertheless, whether increased CaMKII signaling and related SR Ca²⁺ leak contribute to the development of clinical AF remains to be determined.

Clinical implications. Our findings show that CaMKII augmentation of aberrant SR Ca²⁺ release, in conjunction with a tissue or cellular abnormality that promotes AF maintenance, may be one of the multiple mechanisms leading to induction of AF. According to this double-hit concept, the AF substrate could be a genetic mutation (for instance, in RyR2) or atrial remodeling (electrical or structural). Three recent studies have demonstrated evidence for AF under certain circumstances in patients with genetic defects in the *Ryr2* gene (37–39), albeit genetic forms of RyR2-mediated AF are not very common. In addition, enhanced CaMKII phosphorylation of RyR2 was confirmed in atrial biopsies from mice with atrial enlargement and spontaneous AF development, goats with lone AF, and patients with chronic AF. These findings suggest that increased RyR2-dependent Ca²⁺ leak due to enhanced CaMKII activity may be important for the pathogenesis of clinical AF. Our data in *Ryr2^{S2814A}* knockin mice suggest that phosphorylation of S2814 on RyR2 is the major, but presumably not the only, downstream target of CaMKII during AF evolution. CaMKII is a known proarrhythmic signal and a promising therapeutic target for prevention of ventricular arrhythmias and sudden death (57). Our new findings expand the impact and scope of these earlier studies by showing that CaMKII inhibition could be a new approach to treating AF. Finally, the reduction of SR Ca²⁺ leak via defective RyR2 channels, whether genetic or acquired, may constitute a novel strategy to reduce atrial arrhythmogenesis, and reduction in SR Ca²⁺ leak might be possible by inhibition of RyR2-related CaMKII activity. Additional studies in larger mammals and patients with AF are needed to confirm the therapeutic potential of RyR2-based therapies for AF.

Methods

Generation of mouse strains and animal care. Generation of *Ryr2^{R176Q/+}* knockin, AC3-I, and AC3-C transgenic mice was previously described (15, 20). *Ryr2^{R176Q/+}* knockin mice were generously provided by Susan Hamilton. CREM-IbAC-X-overexpressing mice were described previously (29).

Ryr2^{S2814A} knockin mice were generated as shown in Figure 8. In brief, a genomic clone containing exons 56 and 57 of the mouse *Ryr2* gene was isolated from a 129/SvJ λKO-1 library and cloned into a pDTA4B vector using homologous recombination (58). The sequence encoding the S2814A mutation was introduced into exon 56 of *Ryr2*, along with a new ClaI site. A cassette containing a loxP-flanked NeoR gene expressed from the phosphoglycerate kinase promoter (PGK-NeoR) was cloned into intron 56 to obtain the final targeting vector. Targeting vector was linearized with PmeI and electroporated into AB2.2 129Sv/J ES cells. After identification of homologous-targeted integrands using Southern blot analysis, ES cells were injected into blastocysts to generate chimeric mice. Following germline transmission and crossing with Meox2-Cre mice, the final allele without Neo cassette was obtained. Heterozygous *Ryr2^{S2814A}* mice were mated to obtain *Ryr2^{S2814A}* homozygous knockin mice and WT littermates. All animal studies were performed according to protocols approved by the Institutional Animal Care and Use Committee of Baylor College of Medicine and conformed to the *Guide for the care and use of laboratory animals* (NIH Publication no. 85-23. Revised 1996).

ECG telemetry. ECG transmitters (Data Sciences International) were implanted in the abdominal cavity of *Ryr2^{R176Q/+}* mice with subcutaneous electrodes in a lead II configuration (15). ECGs were recorded by telemetry using Dataquest software, version 4.1 (Data Sciences International) for more than 72 hours after surgery in ambulatory, awake mice. Data analyses were performed off-line using Dataquest software.

Intracardiac electrophysiology in mice. Atrial and ventricular intracardiac electrograms were recorded using a 1.1F octapolar catheter (EPR-800; Millar Instruments) inserted via the right jugular vein, as previously described (59). In brief, right atrial pacing was performed using 2-ms current pulses delivered by an external stimulator (STG-3008; Multi Channel Systems). A computer-based data acquisition system (emka TECHNOLOGIES) was used to record a 6-lead body surface ECG and up to 4 intracardiac bipolar electrograms. Surface and intracardiac electrophysiology parameters were assessed at baseline, as described previously (59).

Inducibility of AF was determined using the protocol described by Verheule et al. (17) and was considered positive if at least 2 of 3 pacing trials induced AF. AF was defined as the occurrence of rapid and fragmented atrial electrograms with irregular AV-nodal conduction and ventricular rhythm for at least 1 second. A subset of *Ryr2^{R176Q/+}* mice positive for AF was injected i.p. with the CaMKII inhibitor KN-93 (10–30 μmol/kg) (Calbiochem), the inactive analog KN-92 (10 μmol/kg) (Calbiochem), or placebo (saline) (19). After a 10-minute incubation period, all pacing protocols were repeated. Experiments in *Ryr2^{S2814A}* and WT mice were performed after pacing threshold was determined as described (59). AF inducibility was determined 2 minutes after injection of 50 ng/g carbachol i.p. (Sigma-Aldrich) (30).

Histology. Mice (10 to 14 weeks) were anesthetized using a mixture of 1.5% isoflurane and 95% O₂. After blood was drained from the inferior vena cava, hearts from WT (*n* = 4) and *Ryr2^{R176Q/+}* (*n* = 4) mice were fixed in 4% buffered formaldehyde for 48 hours. After paraffin embedding and sectioning, sections were stained with H&E for cell morphology and Masson trichrome for interstitial fibrosis.

Reverse transcription polymerase chain reaction and Western blot analysis. Gene expression was determined by RT-PCR and Western blotting as previously described (59). Details are provided in Supplemental Materials and Methods.

Ca²⁺ transient measurements. Single atrial myocytes were isolated from the hearts of 3- to 5-month-old WT and *Ryr2^{R176Q/+}* mice using standard enzymatic dissociation as previously described (59). Details are provided in Supplemental Materials and Methods. SR Ca²⁺ leak was measured as described in detail by Shannon et al. (ref. 22; see Supplemental Materials and Methods).



Atrial mapping studies. Dual voltage (V_m) and Ca^{2+} atrial mapping was performed as previously described with modifications (54). Simultaneous signals were recorded with synchronized charge-coupled device (CCD) cameras operating at 0.6 ms per frame with a spatial resolution of 32×32 pixels (0.125×0.125 mm² per pixel). Bipolar stimuli were delivered to the atria at a 5 V output using platinum electrodes and a Grass stimulator (S88X; Grass Technologies) triggered by computer-controlled pacing sequences as (a) steady state 5 Hz pacing for 30 seconds and (b) decremental CL pacing in steps of 20 ms from 200 ms to 120 ms and subsequently in steps of 10 ms down to 70 ms for 2 seconds each. Each pacing protocol was performed in duplicate. Atrial imaging was performed in the presence and absence of 1 μ M KN-93. Data were analyzed with custom software (54). Details of the experimental setup are provided in Supplemental Materials and Methods.

Human atrial samples. Human right atrial appendage biopsies were obtained from patients in sinus rhythm and with chronic AF who had undergone the maze procedure during coronary artery bypass graft surgery. The study was approved by the institutional review committees of Baylor College of Medicine and Dresden University of Technology. All subjects gave informed consent.

Goat atrial samples. AF was induced in 5 chronically instrumented goats by repetitive burst pacing with an Intrel pacemaker (Medtronic) for 10 days as previously described (26).

Statistics. Results are expressed as mean \pm SEM. Data were statistically evaluated by paired 2-tailed Student's *t* test or χ^2 for parametric variables. *P* < 0.05 was considered statistically significant.

Acknowledgments

The authors thank Annett Opitz and Sabine Kirsch for technical support and the surgeons from the Cardiosurgery Department, Dresden University of Technology. X.H.T. Wehrens is supported by a national Scientist Development grant from the American Heart Association (0535310N), an NIH/National Heart Lung and

Blood Institute (NHLBI) grant (R01-HL089598), and a March of Dimes grant (MOD24172). M.G. Chelu is the recipient of the Michael Bilitch Fellowship in Cardiac Pacing and Electrophysiology, 2007–2008, from the Heart Rhythm Society and a Texas Affiliate American Heart Association Postdoctoral Fellowship, 2008–2010. S. Sarma is funded by an NIH/NHLBI training grant (T32-HL007706). M.E. Anderson is supported by NIH grants R01 HL079031, R01 HL62494, and R01 HL70250 and the University of Iowa Research Foundation. D. Dobrev and U. Schotten are supported by the German Federal Ministry of Education and Research through the Atrial Fibrillation Competence Network (grant 01Gi0204; projects C3 through C5). F.U. Müller is supported by the German Research Foundation (DFG Mu 1376-10-3). M.Valderrábano is funded by grants from the NIH/NHLBI (R21 HL085215-01) and the Houston Texans. This project was supported by 2 grants from the Fondation Leducq: the Alliance for Calmodulin Kinase Signaling in Heart Disease (08CVD01 to M.E. Anderson and X.H.T. Wehrens) and the European North American Atrial Fibrillation Research Alliance (07CVD03 to U. Schotten and D. Dobrev).

Received for publication August 6, 2008, and accepted in revised form April 29, 2009.

Address correspondence to: Xander H.T. Wehrens, Department of Molecular Physiology and Biophysics, Baylor College of Medicine, One Baylor Plaza, BCM335, Houston, Texas 77030, USA. Phone: (713) 798-4261; Fax: (713) 798-3475; E-mail: wehrens@bcm.edu. Or to: Dobromir Dobrev, Department of Pharmacology and Toxicology, Dresden University of Technology, Fetscherstrasse 74, 01307 Dresden, Germany. Phone: 49-351-458-6279; Fax: 49-351-458-6315; E-mail: dobrev@rcs.urz.tu-dresden.de.

- Bers, D.M. 2002. Cardiac excitation-contraction coupling. *Nature*. **415**:198–205.
- Wehrens, X.H., Lehnart, S.E., and Marks, A.R. 2005. Intracellular calcium release and cardiac disease. *Annu. Rev. Physiol.* **67**:69–98.
- Hove-Madsen, L., et al. 2004. Atrial fibrillation is associated with increased spontaneous calcium release from the sarcoplasmic reticulum in human atrial myocytes. *Circulation*. **110**:1358–1363.
- Vest, J.A., et al. 2005. Defective cardiac ryanodine receptor regulation during atrial fibrillation. *Circulation*. **111**:2025–2032.
- Van Wagoner, D.R., et al. 1999. Atrial L-type Ca^{2+} currents and human atrial fibrillation. *Circ. Res.* **85**:428–436.
- Christ, T., et al. 2004. L-type Ca^{2+} current downregulation in chronic human atrial fibrillation is associated with increased activity of protein phosphatases. *Circulation*. **110**:2651–2657.
- de Bakker, J.M., Ho, S.Y., and Hocini, M. 2002. Basic and clinical electrophysiology of pulmonary vein ectopy. *Cardiovasc. Res.* **54**:287–294.
- Wehrens, X.H., et al. 2004. Protection from cardiac arrhythmia through ryanodine receptor-stabilizing protein calstabin2. *Science*. **304**:292–296.
- Chelu, M.G., and Wehrens, X.H. 2007. Sarcoplasmic reticulum calcium leak and cardiac arrhythmias. *Biochem. Soc. Trans.* **35**:952–956.
- Balasubramaniam, R., Chawla, S., Grace, A.A., and Huang, C.L. 2005. Caffeine-induced arrhythmias in murine hearts parallel changes in cellular Ca^{2+} homeostasis. *Am. J. Physiol. Heart Circ. Physiol.* **289**:H1584–H1593.
- Venetucci, L.A., Trafford, A.W., and Eisner, D.A. 2007. Increasing ryanodine receptor open probability alone does not produce arrhythmogenic calcium waves: threshold sarcoplasmic reticulum calcium content is required. *Circ. Res.* **100**:105–111.
- Eckstein, J., Verheule, S., de Groot, N., Allesie, M., and Schotten, U. 2008. Mechanisms of perpetuation of atrial fibrillation in chronically dilated atria. *Prog. Biophys. Mol. Biol.* **97**:435–451.
- Nattel, S., Shiroshita-Takeshita, A., Brundel, B.J., and Rivard, L. 2005. Mechanisms of atrial fibrillation: lessons from animal models. *Prog. Cardiovasc. Dis.* **48**:9–28.
- Bauce, B., et al. 2002. Screening for ryanodine receptor type 2 mutations in families with effort-induced polymorphic ventricular arrhythmias and sudden death: early diagnosis of asymptomatic carriers. *J. Am. Coll. Cardiol.* **40**:341–349.
- Kannankeril, P.J., et al. 2006. Mice with the R176Q cardiac ryanodine receptor mutation exhibit catecholamine-induced ventricular tachycardia and cardiomyopathy. *Proc. Natl. Acad. Sci. U. S. A.* **103**:12179–12184.
- Jiang, D., et al. 2005. Enhanced store overload-induced Ca^{2+} release and channel sensitivity to luminal Ca^{2+} activation are common defects of RyR2 mutations linked to ventricular tachycardia and sudden death. *Circ. Res.* **97**:1173–1181.
- Verheule, S., et al. 2004. Increased vulnerability to atrial fibrillation in transgenic mice with selective atrial fibrosis caused by overexpression of TGF- β 1. *Circ. Res.* **94**:1458–1465.
- Wehrens, X.H., Lehnart, S.E., Reiken, S.R., and Marks, A.R. 2004. Ca^{2+} /calmodulin-dependent protein kinase II phosphorylation regulates the cardiac ryanodine receptor. *Circ. Res.* **94**:e61–e70.
- Wu, Y., et al. 2002. Calmodulin kinase II and arrhythmias in a mouse model of cardiac hypertrophy. *Circulation*. **106**:1288–1293.
- Zhang, R., et al. 2005. Calmodulin kinase II inhibition protects against structural heart disease. *Nat. Med.* **11**:409–417.
- Wehrens, X.H., et al. 2003. FKBP12.6 deficiency and defective calcium release channel (ryanodine receptor) function linked to exercise-induced sudden cardiac death. *Cell*. **113**:829–840.
- Shannon, T.R., Ginsburg, K.S., and Bers, D.M. 2002. Quantitative assessment of the SR Ca^{2+} leak-load relationship. *Circ. Res.* **91**:594–600.
- Konings, K.T., Smeets, J.L., Penn, O.C., Wellens, H.J., and Allesie, M.A. 1997. Configuration of unipolar atrial electrograms during electrically induced atrial fibrillation in humans. *Circulation*. **95**:1231–1241.
- Haissaguerre, M., et al. 1998. Spontaneous initiation of atrial fibrillation by ectopic beats originating in the pulmonary veins. *N. Engl. J. Med.* **339**:659–666.
- Nattel, S., Maguy, A., Le Boucq, S., and Yeh, Y.H. 2007. Arrhythmogenic ion-channel remodeling in the heart: heart failure, myocardial infarction, and atrial fibrillation. *Physiol. Rev.* **87**:425–456.
- Schotten, U., et al. 2003. Electrical and contractile remodeling during the first days of atrial fibrillation go hand in hand. *Circulation*. **107**:1433–1439.
- Greiser, M., et al. 2009. Distinct contractile and molecular differences between two goat models of atrial dysfunction: AV block-induced atrial dilatation and atrial fibrillation. *J. Mol. Cell. Cardiol.* **46**:385–394.
- Maier, L.S. 2005. CaMKII δ overexpression in hypertrophy and heart failure: cellular consequences for excitation-contraction coupling. *Braz. J. Med.*



- Biol. Res.* **38**:1293–1302.
29. Muller, F.U., et al. 2005. Heart-directed expression of a human cardiac isoform of cAMP-response element modulator in transgenic mice. *J. Biol. Chem.* **280**:6906–6914.
30. Wakimoto, H., et al. 2001. Induction of atrial tachycardia and fibrillation in the mouse heart. *Cardiovasc. Res.* **50**:463–473.
31. El-Armouche, A., et al. 2006. Molecular determinants of altered Ca^{2+} handling in human chronic atrial fibrillation. *Circulation.* **114**:670–680.
32. Fujiwara, K., Tanaka, H., Mani, H., Nakagami, T., and Takamatsu, T. 2008. Burst emergence of intracellular Ca^{2+} waves evokes arrhythmogenic oscillatory depolarization via the Na^+ - Ca^{2+} exchanger simultaneous confocal recording of membrane potential and intracellular Ca^{2+} in the heart. *Circ. Res.* **103**:509–518.
33. Brundel, B.J., et al. 1999. Gene expression of proteins influencing the calcium homeostasis in patients with persistent and paroxysmal atrial fibrillation. *Cardiovasc. Res.* **42**:443–454.
34. Lai, L.P., et al. 1999. Down-regulation of L-type calcium channel and sarcoplasmic reticular Ca^{2+} -ATPase mRNA in human atrial fibrillation without significant change in the mRNA of ryanodine receptor, calsequestrin and phospholamban: an insight into the mechanism of atrial electrical remodeling. *J. Am. Coll. Cardiol.* **33**:1231–1237.
35. Thijssen, V.L., et al. 2004. Troponin I isoform expression in human and experimental atrial fibrillation. *Circulation.* **110**:770–775.
36. Ohkusa, T., et al. 1999. Alterations in cardiac sarcoplasmic reticulum Ca^{2+} regulatory proteins in the atrial tissue of patients with chronic atrial fibrillation. *J. Am. Coll. Cardiol.* **34**:255–263.
37. Sumitomo, N., et al. 2007. Association of atrial arrhythmia and sinus node dysfunction in patients with catecholaminergic polymorphic ventricular tachycardia. *Circ. J.* **71**:1606–1609.
38. Pizzale, S., Gollob, M.H., Gow, R., and Birnie, D.H. 2008. Sudden death in a young man with catecholaminergic polymorphic ventricular tachycardia and paroxysmal atrial fibrillation. *J. Cardiovasc. Electrophysiol.* **19**:1319–1321.
39. Bhuiyan, Z.A., et al. 2007. Expanding spectrum of human RYR2-related disease: new electrocardiographic, structural, and genetic features. *Circulation.* **116**:1569–1576.
40. Guo, T., Zhang, T., Mestril, R., and Bers, D.M. 2006. Ca^{2+} /Calmodulin-dependent protein kinase II phosphorylation of ryanodine receptor does affect calcium sparks in mouse ventricular myocytes. *Circ. Res.* **99**:398–406.
41. Yurukova, S., et al. 2007. CaMKII-mediated increased lusitropic responses to beta-adrenoreceptor stimulation in ANP-receptor deficient mice. *Cardiovasc. Res.* **73**:678–688.
42. Tessier, S., et al. 1999. Regulation of the transient outward K^+ current by Ca^{2+} /calmodulin-dependent protein kinases II in human atrial myocytes. *Circ. Res.* **85**:810–819.
43. Ai, X., Curran, J.W., Shannon, T.R., Bers, D.M., and Pogwizd, S.M. 2005. Ca^{2+} /calmodulin-dependent protein kinase modulates cardiac ryanodine receptor phosphorylation and sarcoplasmic reticulum Ca^{2+} leak in heart failure. *Circ. Res.* **97**:1314–1322.
44. Zhang, T., et al. 2003. The deltaC isoform of CaMKII is activated in cardiac hypertrophy and induces dilated cardiomyopathy and heart failure. *Circ. Res.* **92**:912–919.
45. Dobrev, D. 2006. Electrical remodeling in atrial fibrillation. *Herz.* **31**:108–112.
46. Shiroshita-Takeshita, A., Brundel, B.J., and Nattel, S. 2005. Atrial fibrillation: basic mechanisms, remodeling and triggers. *J. Interv. Card. Electrophysiol.* **13**:181–193.
47. Honjo, H., et al. 2003. Sarcoplasmic reticulum Ca^{2+} release is not a dominating factor in sinoatrial node pacemaker activity. *Circ. Res.* **92**:e41–e44.
48. Patterson, E., et al. 2007. Spontaneous pulmonary vein firing in man: relationship to tachycardia-pause early afterdepolarizations and triggered arrhythmia in canine pulmonary veins in vitro. *J. Cardiovasc. Electrophysiol.* **18**:1067–1075.
49. Patterson, E., Po, S.S., Scherlag, B.J., and Lazzara, R. 2005. Triggered firing in pulmonary veins initiated by in vitro autonomic nerve stimulation. *Heart Rhythm.* **2**:624–631.
50. Chen, Y.J., Chen, Y.C., Wongcharoen, W., Lin, C.I., and Chen, S.A. 2008. Effect of K201, a novel antiarrhythmic drug on calcium handling and arrhythmogenic activity of pulmonary vein cardiomyocytes. *Br. J. Pharmacol.* **153**:915–925.
51. Scherlag, B.J., et al. 2008. An acute model for atrial fibrillation arising from a peripheral atrial site: evidence for primary and secondary triggers. *J. Cardiovasc. Electrophysiol.* **19**:519–527.
52. Burashnikov, A., and Antzelevitch, C. 2003. Reinduction of atrial fibrillation immediately after termination of the arrhythmia is mediated by late phase 3 early afterdepolarization-induced triggered activity. *Circulation.* **107**:2355–2360.
53. Xie, L.H., Chen, F., Karagueuzian, H.S., and Weiss, J.N. 2008. Oxidative stress-induced afterdepolarizations and calmodulin kinase II signaling. *Circ. Res.* **104**:79–86.
54. de Diego, C., et al. 2008. Cardiac alternans in embryonic mouse ventricles. *Am. J. Physiol. Heart Circ. Physiol.* **294**:H433–H440.
55. Patterson, E., et al. 2006. Sodium-calcium exchange initiated by the Ca^{2+} transient: an arrhythmia trigger within pulmonary veins. *J. Am. Coll. Cardiol.* **47**:1196–1206.
56. Chou, C.C., et al. 2005. Intracellular calcium dynamics and anisotropic reentry in isolated canine pulmonary veins and left atrium. *Circulation.* **111**:2889–2897.
57. Khoo, M.S., et al. 2006. Death, cardiac dysfunction, and arrhythmias are increased by calmodulin kinase II in calcineurin cardiomyopathy. *Circulation.* **114**:1352–1359.
58. Zhang, P., Li, M.Z., and Elledge, S.J. 2002. Towards genetic genome projects: genomic library screening and gene-targeting vector construction in a single step. *Nat. Genet.* **30**:31–39.
59. Sood, S., et al. 2008. Intracellular calcium leak due to FKBP12.6 deficiency in mice facilitates the inducibility of atrial fibrillation. *Heart Rhythm.* **5**:1047–1054.